Pex3 peroxisome biogenesis proteins function in peroxisome inheritance as class V myosin receptors

Jinlan Chang, Fred D. Mast, Andrei Fagarasanu, Dorian A. Rachubinski, Gary A. Eitzen, Joel B. Dacks, and Richard A. Rachubinski

Department of Cell Biology, University of Alberta, Edmonton, Alberta T6G 2H7, Canada

In *Saccharomyces cerevisiae*, peroxisomal inheritance from mother cell to bud is conducted by the class V myosin motor, Myo2p. However, homologues of *S. cerevisiae* Myo2p peroxisomal receptor, Inp2p, are not readily identifiable outside the *Saccharomycetaceae* family. Here, we demonstrate an unexpected role for Pex3 proteins in peroxisome inheritance. Both Pex3p and Pex3Bp are peroxisomal integral membrane proteins that function as peroxisomal receptors for class V myosin through direct interaction with the myosin globular tail. In cells lacking Pex3Bp, peroxisomes are preferentially retained by the mother cell, whereas most peroxisomes gather and are transferred en masse to the bud in cells overexpressing Pex3Bp or Pex3p. Our results reveal an unprecedented role for members of the Pex3 protein family in peroxisome motility and inheritance in addition to their well-established role in peroxisome biogenesis at the endoplasmic reticulum. Our results point to a temporal link between peroxisome formation and inheritance and delineate a general mechanism of peroxisome inheritance in eukaryotic cells.

Introduction

Peroxisomes are ubiquitous organelles found in diverse eukaryotic organisms and cell types. They function in fatty acid metabolism and the detoxification of reactive oxygen species. Peroxisomes are generally spherical, delimited by a single membrane, and contain a fine granular matrix. Unlike mitochondria and chloroplasts, peroxisomes do not contain DNA or an independent protein synthesis machinery, and thus all peroxisomal proteins are encoded in the nucleus and synthesized on cytoplasmic polysomes. The essential requirement for peroxisomes is underscored by the existence of several fatal genetic disorders, collectively called the peroxisome biogenesis disorders (PBDs), in which peroxisome assembly is compromised (for classical and current views of peroxisomes, their functions, and the diseases associated with them, see Lazarow and Fujiki, 1985; van den Bosch et al., 1992; Steinberg et al., 2006; Wanders and Waterham, 2006; Schrader and Fahimi, 2008).

Given the importance of peroxisomes for normal cell physiology and the catastrophic health consequences of loss of peroxisomal function, molecular mechanisms have evolved to ensure the continuity of the peroxisome population during multiple rounds of cell division. When cells divide, they double the number of their peroxisomes and distribute them equitably between the two resulting cells. Peroxisome duplication can be achieved by two distinct pathways: growth and division of preexisting peroxisomes and de novo synthesis.

The ability of peroxisomes to form de novo suggested that another organelle must provide peroxisomal membrane components. Both morphological and biochemical evidence suggested a role for the ER as the donor compartment (Novikoff and Shin, 1964; Novikoff and Novikoff, 1972; Titorenko et al., 1997, 2000; Titorenko and Rachubinski, 1998; Geuze et al., 2003). However, an ER origin for peroxisomes remained controversial (Lazarow, 2003) until studies in *Saccharomyces cerevisiae* provided incontrovertible evidence that the ER is indeed the site of de novo peroxisome biogenesis (Hoepfner et al., 2005; Tam et al., 2005). These studies showed that the integral peroxisomal membrane protein (PMP), Pex3p, targets to discrete ER-localized punctae, forming a dynamic ER subcompartment en route to the peroxisome. Pex3p has been shown to play an essential role in peroxisome biogenesis in the cells of a variety of organisms. Pex3p acts to dock Pex19p, a peroxin that functions as a receptor

Correspondence to Richard Rachubinski: rick.rachubinski@ualberta.ca

Abbreviations used in this paper: BLAST, Basic Local Alignment Search Tool; MBP, maltose-binding protein; ORF, open reading frame; PMP, peroxisomal membrane protein; PNS, postnuclear supernatant.

The Rockefeller University Press $30.00
J. Cell Biol. Vol. 187 No. 2 233–246
www.jcb.org/cgi/doi/10.1083/jcb.200902117

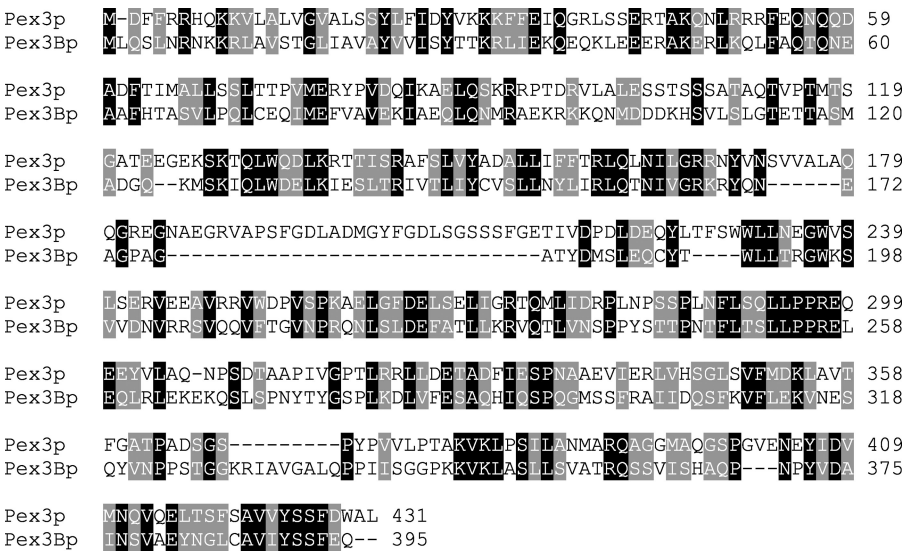

Figure 1. **Sequence alignment of Pex3p with the hypothetical protein Pex3Bp encoded by the *Y. lipolytica* genome.** Amino acid sequences were aligned with the use of the ClustalW program (EMBL-EBI; http://www.ebi.ac.uk/Tools/clustalw2). Identical residues (black) and similar residues (gray) in the two proteins are shaded. Similarity rules: G = A = S; A = V; V = I = L = M; I = L = M = F = Y = W; K = R = H; D = E = Q = N; and S = T = Q = N. Dashes represent gaps. Amino acid numbers are shown on the right.

and/or chaperone for PMPs. Cells lacking Pex3p or Pex19p are devoid not only of mature peroxisomes but also of any peroxisomal remnants (for a review of Pex3p and its functions and interactions, see Fujiki et al., 2006).

However, it has recently been shown that peroxisome number is maintained in wild-type *S. cerevisiae* cells by growth and division of preexisting peroxisomes rather than de novo synthesis of peroxisomes from the ER (Motley and Hettema, 2007). Only *S. cerevisiae* cells that have lost peroxisomes because of a partitioning defect were observed to manufacture peroxisomes anew. Therefore, at least in *S. cerevisiae*, the function of the ER-to-peroxisome pathway must normally be to supply existing peroxisomes with membrane components to allow them to sustain multiple rounds of growth and division. The successful inheritance of peroxisomes has been shown to be accomplished by the transport of about half of the peroxisomes to the growing bud, concomitant with the active retention of the remaining peroxisomes in the mother cell (Fagarasanu et al., 2005). Peroxisomes in *S. cerevisiae* are propelled by the class V myosin motor, Myo2p, which attaches to the peroxisomal membrane via the integral PMP, Inp2p (Fagarasanu et al., 2006). However, no Inp2p homologues are readily identifiable outside the *Saccharomycetaceae* family, which raises important questions about the conservation of the mechanism of peroxisome inheritance.

The yeast *Yarrowia lipolytica* is unique among organisms with completed genome sequences in having a paralogue of Pex3p, termed Pex3Bp (Fig. 1; Kiel et al., 2006), whose role in peroxisome biogenesis and function, if any, is unknown. In this study, we show that Pex3Bp is an integral PMP that acts as a peroxisome-specific receptor for the class V myosin motor that traffics peroxisomes along actin to daughter cells and also functions in regulating peroxisome structure and morphology. We also show that Pex3p itself can bind myosin V and function in peroxisome inheritance. As the Pex3 family is highly conserved throughout the eukaryotes, our findings delineate a general mechanism for peroxisome inheritance and point to a temporal link between peroxisome formation and inheritance, with the appealing possibility that new peroxisomal material is preferentially transferred to daughter cells.

Results

The genome of *Y. lipolytica* encodes a paralogue of Pex3p designated Pex3Bp

Pex3 proteins are peroxisomal integral membrane proteins that act early in the peroxisome biogenic cascade. A search of protein databases using the Basic Local Alignment Search Tool (BLAST) program of the National Center for Biotechnology Information showed that *Y. lipolytica* is unique in having both Pex3p and a paralogue of Pex3p (available from GenBank/EMBL/DDBJ under accession no. XP_501103). This uncharacterized paralogue of Pex3p has previously been designated as Pex3Bp (Kiel et al., 2006), and this convention is retained here. Pex3Bp is predicted to be 395 amino acids in length, 36 amino acids shorter than Pex3p, with a molecular mass of 44,350 D (Fig. 1). Pex3p and Pex3Bp share 29.8% amino acid identity and 26.2% amino acid similarity. Like Pex3p between amino acids 11–28, Pex3Bp is predicted to have one transmembrane domain between amino acids 12 and 30 (http://www.cbs.dtu.dk/services/TMHMM-2.0/).

Pex3Bp is an integral membrane protein of peroxisomes

Because of the extensive similarity between Pex3p and Pex3Bp, we examined whether Pex3Bp, like Pex3p, is localized to peroxisomes. We showed using confocal microscopy that a chimera of Pex3Bp tagged at its C terminus with monomeric red fluorescent protein (Pex3Bp-mRFP) colocalized with a GFP-tagged chimera of the peroxisomal matrix protein thiolase (Pot1p-GFP) to punctate structures characteristic of peroxisomes (Fig. 2 A). Subcellular fractionation showed that Pex3Bp-mRFP, like Pot1p, localized preferentially to a 20,000 *g* pellet fraction (20KgP) enriched for peroxisomes and not a 20,000 *g* supernatant fraction (20KgS) enriched for cytosol (Fig. 2 B). Peroxisomes in the 20KgP fraction were hypotonically lysed by incubation in dilute alkali Tris buffer and subjected to centrifugation to yield a supernatant (Ti8S) enriched for matrix proteins and a pellet (Ti8P) enriched for membrane proteins (Fig. 2 C).

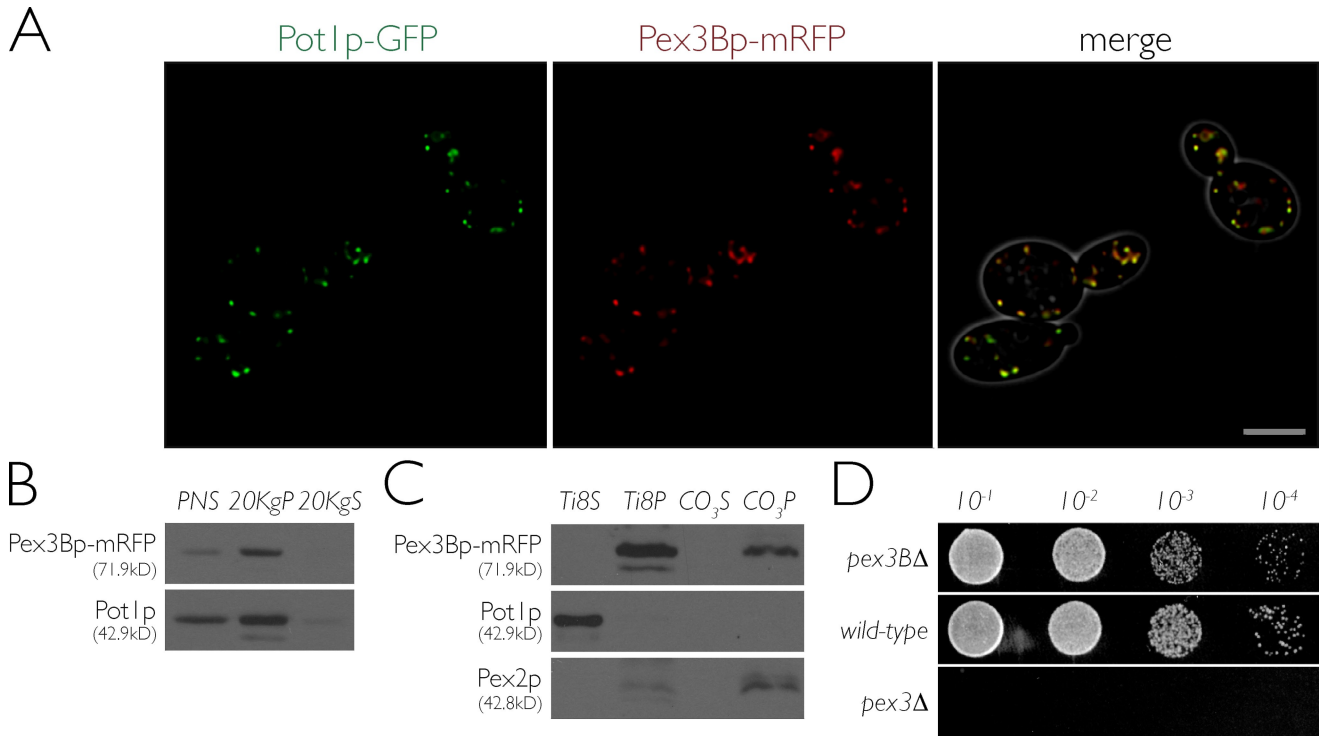

Figure 2. **Pex3Bp is a peroxisomal integral membrane protein.** (A) Pex3Bp-mRFP colocalizes with the peroxisomal chimeric reporter Pot1p-GFP to punctate structures characteristic of peroxisomes by confocal microscopy. The right panel presents the merged image of the left and middle panels, with colocalization of Pex3Bp-mRFP and Pot1p-GFP shown in yellow. Bar, 5 µm. (B) Pex3Bp-mRFP localizes to the 20KgP subcellular fraction enriched for peroxisomes. Immunoblot analysis of equivalent portions of the PNS, 20KgP, and 20KgS subcellular fractions from cells expressing Pex3Bp-mRFP was performed with antibodies to mRFP and to the peroxisomal matrix enzyme thiolase (Pot1p). (C) Pex3Bp exhibits the characteristics of an integral membrane protein. The 20KgP fraction from cells expressing Pex3Bp-mRFP was treated with Ti8 buffer to lyse peroxisomes and then subjected to centrifugation to yield a supernatant fraction (Ti8S) enriched for matrix proteins and a pellet fraction (Ti8P) enriched for membrane proteins. The Ti8P fraction was further treated with alkali Na_2CO_3 and separated by centrifugation into a supernatant fraction (CO_3S) enriched for peripheral membrane proteins and a pellet fraction (CO_3P) enriched for integral membrane proteins. Equivalent portions of each fraction were analyzed by immunoblotting. Immunodetection of Pot1p and Pex2p marked the fractionation profiles of a peroxisomal matrix and integral membrane protein, respectively. (D) *pex3BΔ* cells exhibit slightly retarded growth on oleic acid medium. Cells of the wild-type strain *E122* and of the deletion strains *pex3BΔ* and *pex3Δ* were grown to mid-log phase in liquid YPD, incubated in liquid YPBO for 1 d, spotted at dilutions of 10^{-1}–10^{-4} on YPBO agar, and grown for 2 d at 30°C.

Pex3Bp-mRFP localized almost exclusively to the Ti8P fraction like the known peroxisomal integral membrane protein Pex2p (Eitzen et al., 1996) and in contrast to the soluble peroxisomal matrix enzyme Pot1p, which was found only in the Ti8S fraction. The Ti8P fractions were then extracted with alkali sodium carbonate and subjected to centrifugation (Fig. 2 C). This treatment releases proteins associated with, but not integral to, membranes (Fujiki et al., 1982). Under these conditions, Pex3Bp-mRFP fractionated with Pex2p to the pellet fraction enriched for integral membrane proteins. Isopycnic density gradient centrifugation of the 20KgP fraction indicated that Pex3Bp coenriched with Pot1p and not with the mitochondrial protein Sdh2p (Fig. S1). Collectively, these data demonstrate that Pex3Bp is an integral membrane protein of peroxisomes.

The potential for functional redundancy between Pex3p and Pex3Bp may have prevented the identification of Pex3Bp as a bona fide peroxin that is involved in peroxisome biogenesis in *Y. lipolytica*, which was determined in screens using random mutagenesis and negative selection for growth on medium containing oleic acid as the sole carbon source and whose metabolism requires functional peroxisomes. Consistent with this possibility, the deletion strain *pex3BΔ* was only marginally retarded in growth compared with the wild-type strain *E122* when spotted as serial dilutions onto agar medium containing oleic acid (Fig. 2 D). This is in stark contrast to the *pex3Δ* strain, which shows no growth. The slightly retarded growth of the *pex3BΔ* strain in the presence of oleic acid is consistent with a possible regulatory role in peroxisome morphology, division, or inheritance rather than in peroxisome assembly by itself (Yan et al., 2008).

Deletion of the *PEX3B* gene affects peroxisome morphology

To investigate a possible role for Pex3Bp in peroxisome biogenesis, we used confocal microscopy to track both the subcellular localization of the fluorescent peroxisomal marker chimera Pot1p-GFP and the appearance of peroxisomes containing Pot1p-GFP in *pex3BΔ* cells. Wild-type cells and *pex3BΔ* cells were observed over time after a shift from glucose-containing medium to oleic acid–containing medium. Peroxisomes increase in size and number with a switch from a fermentative carbon source like glucose to a nonfermentative carbon source like oleic acid, which is metabolized exclusively by peroxisomes.

At the time of transfer from glucose-containing to oleic acid–containing medium, wild-type cells had numerous (~20–40) punctate peroxisomes that increased both in size and number with time of incubation in oleic acid–containing medium (Fig. 3 A).

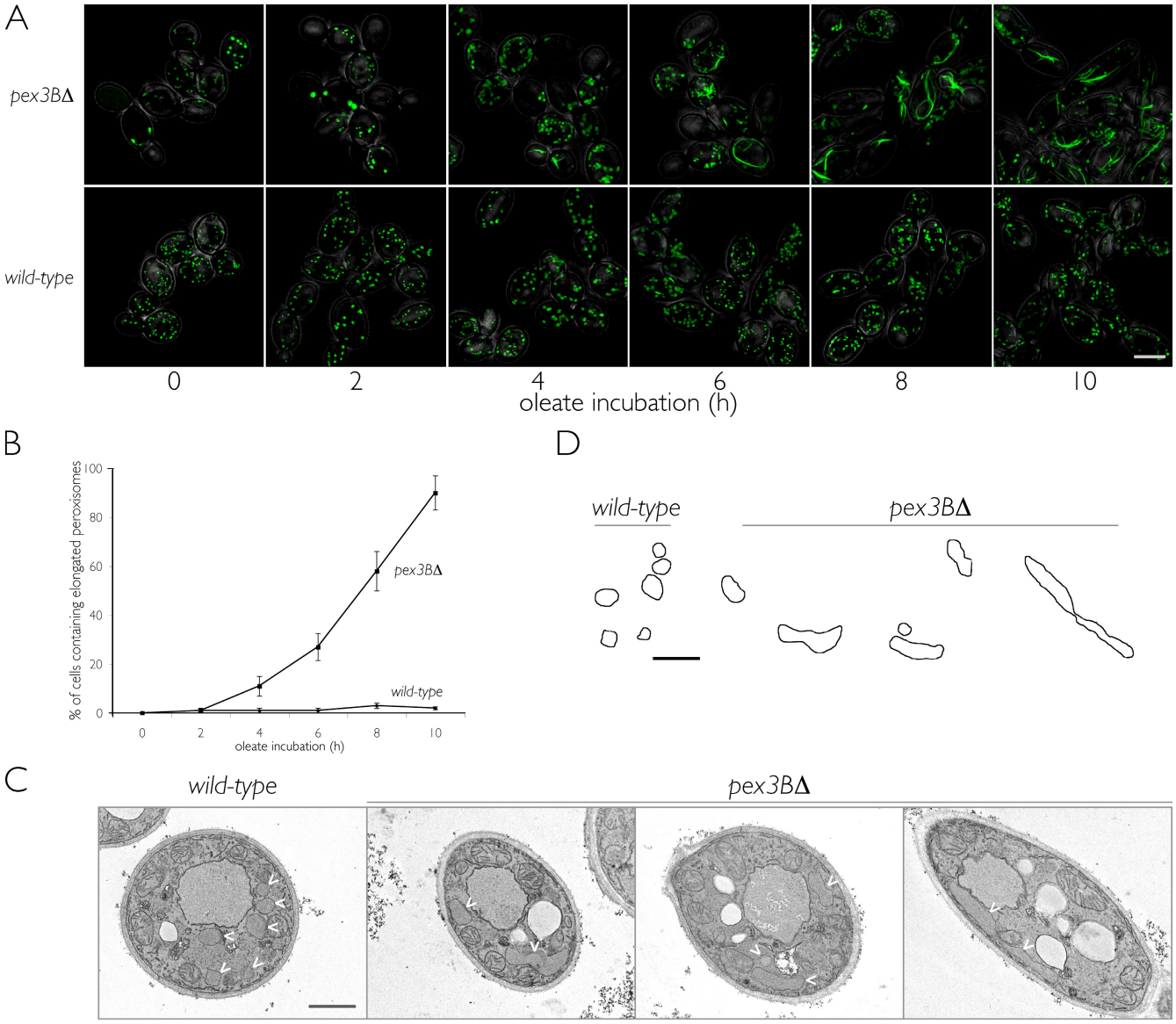

Figure 3. **Deletion of the *PEX3B* gene affects peroxisome morphology.** (A) Wild-type and *pex3BΔ* cells expressing genomically integrated *POT1-GFP* were grown in glucose-containing YPD for 16 h and then transferred to oleic acid–containing YPBO. Fluorescent images of cells at different times of incubation in YPBO were captured by confocal microscopy and deconvolved. Bar, 5 µm. (B) Cells lacking Pex3Bp contain elongated peroxisomes. An elongated peroxisome was functionally defined as being 2 µm or greater in length along its long axis. Graphic results are the means and SEM of three independent experiments. (C) Ultrastructure of wild-type *E122* and *pex3BΔ* cells. Cells were cultured in YPD for 16 h, transferred to YPBO for 10 h, and then fixed and processed for EM. Arrowheads indicate Individual peroxisomes. Bar, 1 µm. (D) Tracings of individual peroxisomes in the electron micrographs of cells presented in C. Bar, 1 µm.

In contrast, the morphology and numbers of peroxisomes were highly heterogenous in *pex3BΔ* cells. As the time of incubation in oleic acid increased, *pex3BΔ* cells exhibited hyperelongated, tubular-reticular peroxisomes, which suggests an imbalance between peroxisome growth and fission in *pex3BΔ* cells. Peroxisome number in *pex3BΔ* cells varied from as low as 1–2 peroxisomes per cell to numbers of peroxisomes comparable to those observed in wild-type cells. The percentage of *pex3BΔ* cells containing elongated peroxisomes increased with time of incubation in oleic acid–containing medium, so that by 10 h of incubation in YPBO, >90% of *pex3BΔ* cells contained tubular-reticular peroxisomes (Fig. 3 B). The percentage of wild-type cells containing elongated peroxisomes never exceeded 1–2%. Furthermore, the reduced numbers of peroxisomes and the elongated peroxisome morphology seen in *pex3BΔ* cells correlated with a noticeable absence of peroxisomes from bud tips in these cells. Thin section transmission EM showed the typical spherical peroxisomal profiles of wild-type cells (Fig. 3, C and D). In contrast, *pex3BΔ* cells contained peroxisomes that were vermiform in appearance and were reduced in number, with typically one or two peroxisomal profiles observed per section as compared with five or more profiles in a section of a wild-type cell (Fig. 3, C and D). The elongated peroxisomes in *pex3BΔ* cells often exhibited a long/short axis ratio in excess of 10:1. These elongated peroxisomes differ in appearance from other elongated peroxisomes previously observed: for example, in *S. cerevisiae* cells lacking the dynamin-related protein

Vps1p, which contain elongated peroxisomes with a beads-on-a-string appearance (Hoepfner et al., 2001); or *S. cerevisiae* cells overexpressing the PMP Pex11p controlling peroxisomal division, which often show two peroxisomes connected by a thin tubule, somewhat like a dumbbell (Erdmann and Blobel, 1995).

Cells lacking Pex3Bp are compromised in peroxisome inheritance

The absence of punctate peroxisomes in many of the bud tips of *pex3BΔ* cells (Figs. 3 A and 4 A) led us to speculate that Pex3Bp might have a role in partitioning peroxisomes between mother cell and bud at cell division. We previously showed that peroxisome inheritance in *Y. lipolytica* is an active process, with protein-mediated retention of peroxisomes in cells and directed transport of peroxisomes along actin filaments to growing buds (Chang et al., 2007). We quantified a defect in peroxisome inheritance in *pex3BΔ* cells (Fig. 4 A). When *pex3BΔ* cells were incubated in oleic acid–containing YPBO medium for 2 h, only 3%, 13%, 19%, and 26% of bud tips in the respective categories I, II, III, and IV (from smallest to largest in size) contained peroxisomes. In wild-type cells, 81% of bud tips in category I and 100% of bud tips in categories II, III, and IV contained peroxisomes. Lack of Pex3Bp specifically affected the inheritance of peroxisomes, as both vacuoles and mitochondria showed normal inheritance in *pex3BΔ* cells (Fig. 4 B). Actin organization in wild-type and *pex3BΔ* cells was similar, with rhodamine-phalloidin staining showing actin patches at sites of polarized growth in both wild-type and *pex3BΔ* cells (Fig. 4 B).

Peroxisome dynamics in *pex3BΔ* cells

Our observations suggested a link between altered peroxisome morphology and defective peroxisome inheritance in *pex3BΔ* cells. We investigated this possible link by imaging wild-type and *pex3BΔ* cells expressing *POT1-GFP* by 4D confocal microscopy (Fig. 5). Peroxisomes in wild-type cells were static or exhibited both directed and saltatory movements (Fig. 5 A and Video 1; Chang et al., 2007). Peroxisome inheritance occurred soon after bud formation, with peroxisomes being delivered to the bud and becoming associated with bud tips. Retrograde movement of peroxisomes from bud to mother could also be detected, and the traffic of peroxisomes between mothers and buds remained bidirectional until cytokinesis, whereupon a new bud emerged and the cycle continued. The saltatory movement of peroxisomes was more apparent in buds than mothers. Peroxisome partitioning led to all mothers and buds having a random distribution of peroxisomes along their cortex, with some peroxisomes being mobile and others being anchored.

In *pex3BΔ* cells, peroxisomes lacked saltatory movements, and their inheritance was delayed or abolished (Fig. 5 B and Video 2). Peroxisomes did not enter the bud until it was approximately half the size of the mother cell, and quickly ceased their movements in the bud, failing to reach the bud tip. Many peroxisomes in *pex3BΔ* cells also became elongated, assumed a tubular-reticular appearance, and were either anchored to the cell cortex or found sliding along the cortex. The elongated peroxisomal phenotype appeared to be a direct consequence of the peroxisome inheritance defect, as elongated peroxisomes were typically

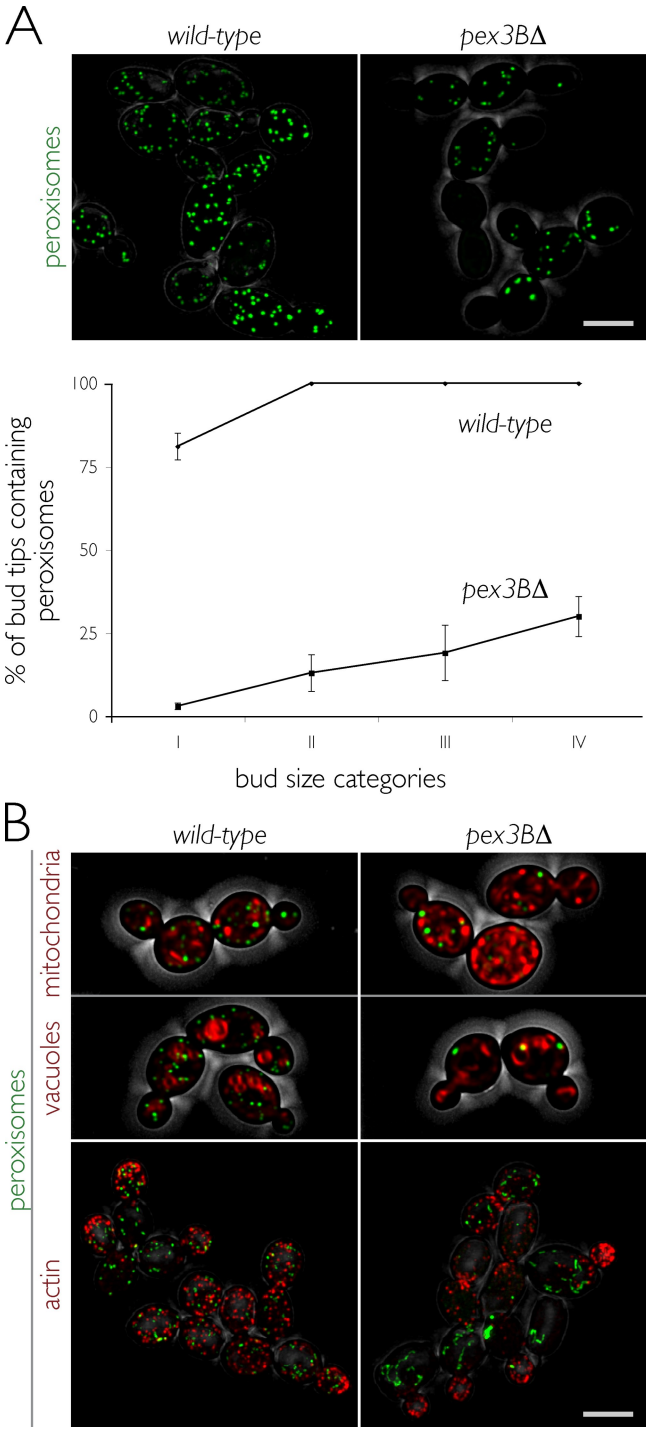

Figure 4. **Deletion of the *PEX3B* gene affects peroxisome inheritance.** (A) Wild-type and *pex3BΔ* cells expressing genomically integrated *POT1-GFP* were grown in YPD for 16 h and then transferred to YPBO for 2 h. Fluorescent images of randomly chosen fields of cells were acquired as a stack by confocal microcopy and deconvolved. Buds were sized according to four categories relative to the volume of the mother cell (see Materials and methods). The percentages of bud tips containing peroxisomes at each size category were plotted. Quantification was performed on at least 50 budded cells from each category. Graphic results are the means and SEM of three independent experiments. Bar, 5 μm. (B) Deletion of the *PEX3B* gene does not affect the actin structure of cells or the inheritance of vacuoles or mitochondria. Wild-type and *pex3BΔ* cells synthesizing Pot1p-GFP were grown in YPD. Mitochondria were stained with Mitotracker dye, vacuoles were stained with the fluorophore FM4-64, and actin was stained with rhodamine-phalloidin. Images were captured by confocal microscopy. Bar, 5 μm.

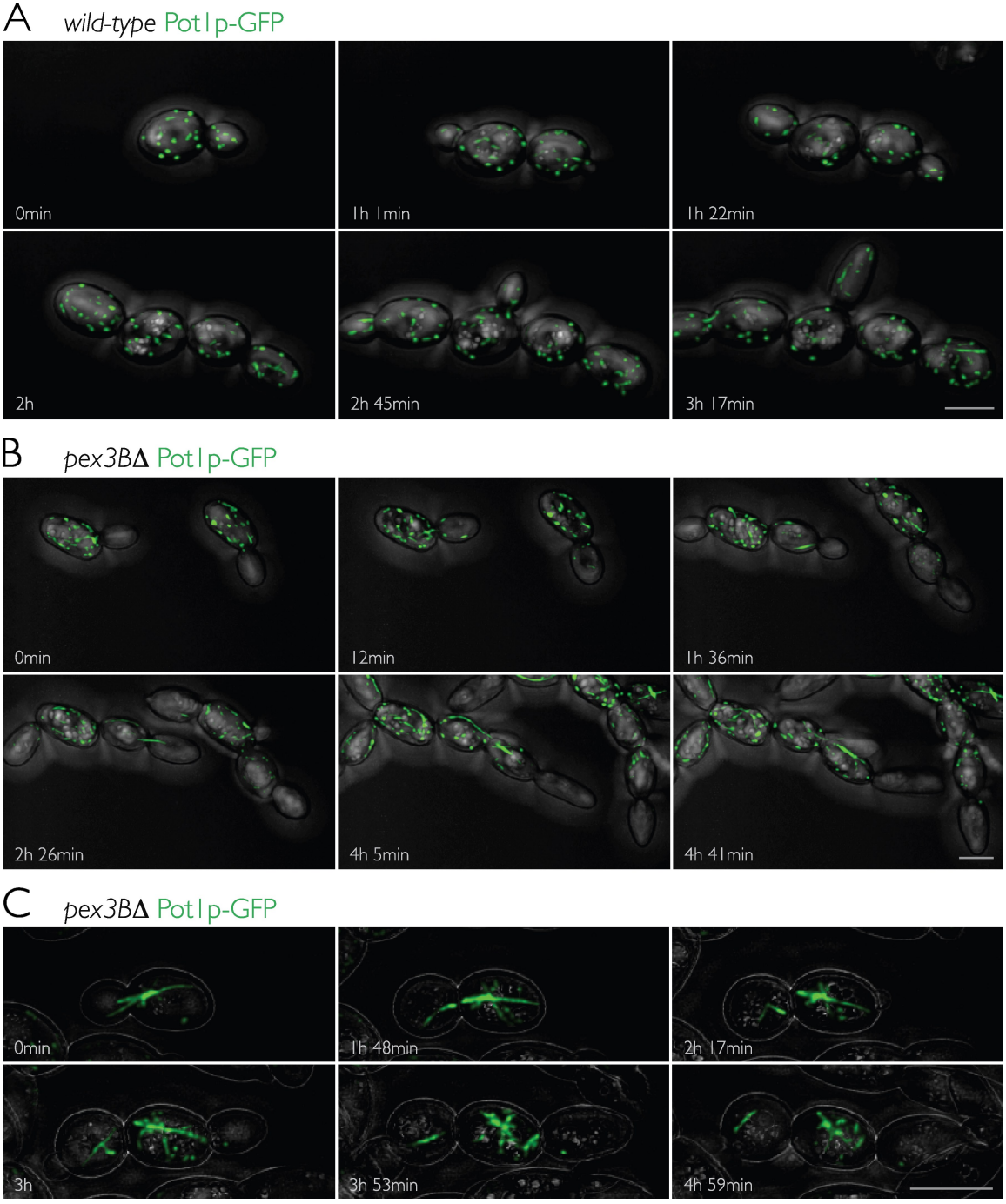

Figure 5. **Peroxisome dynamics and morphogenesis in wild-type and *pex3BΔ* cells visualized by 4D in vivo video microscopy.** Peroxisomes were fluorescently labeled with genomically encoded Pot1p-GFP. Cells were grown for 16 h in YPD, transferred to YPBO for 6 h, and visualized at 28°C (A and B) or 23°C (C) with an LSM 510 confocal microscope specifically modified for 4D in vivo microscopy (see Materials and methods). (A) Wild-type *E122/POT1-GFP* strain. Representative frames from Video 1 show the specific movements and division of peroxisomes through several cell divisions. The emergence of new buds at 1 h 1 min, 1 h 22 min, and 2 h 45 min is followed by the vectorial transfer of a portion of the mother cell's peroxisomes to the bud, where they associate with the bud tip. Bar, 5 µm. (B and C) *pex3BΔ/POT1-GFP* strain. (B) Representative frames from Video 2 display the specific movements and morphogenesis of peroxisomes in *pex3B* cells. At 0 min, both buds lack peroxisomes. By 12 min, several peroxisomes have entered the buds but have failed to associate with the bud tips. Subsequently, many peroxisomes undergo a morphogenic transition, becoming elongated and tubular-reticular in appearance. These peroxisomes often straddle the mother-bud neck (2 h 26 min). Also, peroxisome inheritance does not keep pace with cell division, as many buds are devoid of peroxisomes at later time points (4 h 5 min). Bar, 5 µm. (C) Representative frames from Video 3 display the inability of a tubular-reticular peroxisome to divide except through cytokinesis. A tubular reticular peroxisome is seen initially straddling the mother-bud neck (0 min). At 1 h 48 min, the peroxisome is cut in two by constriction of the septin ring, concluding cytokinesis. A second scission event occurs at 3 h with the conclusion of cytokinesis between the mother cell and the bud to her right. Subsequent buds fail to inherit peroxisomes (4 h 49 min). Bar, 5 µm.

found straddling the mother–bud neck junction, perhaps in an attempt by *pex3BΔ* cells to compensate for their defect in peroxisome inheritance. We also observed that the elongated peroxisomes in *pex3BΔ* cells rarely divided but rather were severed by cytokinesis because of their straddling the mother–bud junction (Fig. 5 C and Video 3). Interestingly, the peroxisome inheritance defect in *pex3BΔ* cells led to buds lacking peroxisomes but now exhibiting de novo peroxisome biogenesis (Video 2). Pot1p-GFP accumulated cytosolically in these buds and then was imported into discrete, newly formed punctae.

Y. lipolytica uses a class V myosin motor to move peroxisomes to buds

Class V myosins are conserved motor proteins that associate with the actin cytoskeleton through their N-terminal motor domain and with the cargo they transport through their C-terminal globular domain. *S. cerevisiae* has two class V myosins, Myo2p and Myo4p. Most organelles, including peroxisomes, are carried to the bud by Myo2p. A search of the *Y. lipolytica* genome revealed one class V myosin encoded by the open reading frame (ORF), *YALI0E00176g*. This class V myosin functions in peroxisome transport to buds, as overexpression of its cargo-binding domain (amino acids 1,092–1,594) led to large reductions in the number of peroxisomes transferred from mother cell to bud (Fig. 6 A). In overexpressing cells, only 25% of small buds and 62% of large buds contained peroxisomes, whereas 90% of small buds and 100% of large buds of wild-type cells contained peroxisomes (Fig. 6 A). Interestingly, overexpressing cells grew more slowly than wild-type cells (unpublished data), which suggests that the unique class V myosin in *Y. lipolytica* may be involved in the transport of other organelles, including secretory vesicles, which are also carried by Myo2p in *S. cerevisiae* (Pashkova et al., 2006).

Pex3Bp interacts directly with the globular tail of the *Y. lipolytica* class V myosin

We performed split-ubiquitin membrane yeast two-hybrid analysis to test the ability of Pex3Bp to interact with the globular tail domain (amino acids 1,092–1,594) of the *Y. lipolytica* class V myosin (Fig. 6 B). A strong interaction was detected between Pex3Bp and the globular tail domain of the class V myosin. Interestingly, Pex3p also showed a detectable interaction. Interactions between Pex3Bp and Pex3p, Pex3Bp and itself, and Pex3p and itself were also observed.

If Pex3Bp is a bona fide peroxisomal receptor for the *Y. lipolytica* class V myosin, we expect it to interact directly with the class V myosin. Because two-hybrid analysis does not differentiate between direct and bridged protein interactions, we performed a pull-down assay using recombinant Pex3Bp and Pex3p fused to maltose-binding protein (MBP) and the *Y. lipolytica* class V myosin tail fused to GST made in *Escherichia coli* (Fig. 6 C). MBP-Pex3Bp was pulled down by the GST–*Y. lipolytica* myosin V (GST-YlMyoV). MBP-Pex3Bp was also pulled down by a GST fusion to the tail domain of *S. cerevisiae* class V myosin, Myo2p (GST-ScMyoV), but to a lesser extent than by GST-YlMyoV. Appreciable amounts of MBP-Pex3p were also pulled down by both GST-YlMyoV and GST-ScMyoV; however, this interaction was not as great as that observed between MBP-Pex3Bp and GST-YlMyoV or GST-ScMyoV. These findings confirmed the results of yeast two-hybrid analysis and ruled out a requirement for additional proteins in the interaction between Pex3Bp or Pex3p and myosin V.

Delivery of peroxisomes from mother cell to bud by an actin-myosin–based system mediated through the interactions of myosin V with Pex3Bp suggested to us that overexpression of Pex3Bp should result in the disproportionate segregation of peroxisomes to the bud, as has been observed for overexpression of the peroxisomal class V myosin receptor, Inp2p, in *S. cerevisiae* (Fagarasanu et al., 2006). To test this prediction, we used 4D confocal microscopy to image *pex3BΔ* cells containing fluorescently labeled peroxisomes and overexpressing *PEX3B* (Fig. 6 D). Rather than the elongated tubular-reticular peroxisomes observed in *pex3BΔ* cells, peroxisomes in cells overexpressing *PEX3B* appeared bulbous and globular (Figs. 6 D and 8 A, and Video 4). These peroxisomes clustered initially near the bud neck region and, despite their large size, were successively delivered through several cell divisions to each newly formed bud. We also detected de novo peroxisome formation occurring in the mother cells devoid of peroxisomes (Video 4). Surprisingly, these de novo made peroxisomes were also transferred to newly formed buds, demonstrating the fidelity of the mechanism of peroxisome inheritance. Our data confirm the role of Pex3Bp in peroxisome inheritance as a peroxisomal receptor for myosin V.

The interaction of Pex3Bp and Pex3p with myosin V was surprising, as we had previously shown that peroxisomes in *S. cerevisiae* are transported by the myosin V motor protein, Myo2p, through its direct interaction with Inp2p (Fagarasanu et al., 2006). Inp2p shows no obvious homology to Pex3Bp (unpublished data). We therefore searched the *Y. lipolytica* genome for a possible Inp2p orthologue. A position-specific iterated BLAST (Altschul et al., 1997) of three iterations using the *S. cerevisiae* protein Inp2p as a bait sequence identified the protein encoded by the ORF *YALI0E03124g* as a possible Inp2p orthologue in *Y. lipolytica*. We tested YALI0E03124p for two critical attributes of a peroxisome-specific receptor for myosin V: direct interaction with myosin V and specific localization to peroxisomes. In a pull-down assay, recombinant MBP-YALI0E03124p did not interact with GST-YlMyoV (Fig. 6 C), ruling out a direct interaction between the two proteins. Furthermore, YALI0E03124p did not localize to peroxisomes and, under conditions in which cells were incubated in oleic acid, was targeted to regions of the cell that appeared to be elements of the secretory pathway (Fig. 7). Thus, peroxisomal recognition of myosin V in *Y. lipolytica* is done primarily by Pex3Bp but also by Pex3p.

Pex3p can function as the peroxisome-specific receptor for myosin V in *pex3BΔ* cells

To better understand the relationship between Pex3p and Pex3Bp and to further explore their relative functions in peroxisome biogenesis and/or in modulating peroxisome morphology and inheritance, Pex3p and Pex3Bp were reciprocally overexpressed in cells of their respective deletion backgrounds. Cells harboring plasmids encoding *PEX3* or *PEX3B* under the control of the oleic acid–inducible *POT1* promoter were incubated in oleic acid–containing

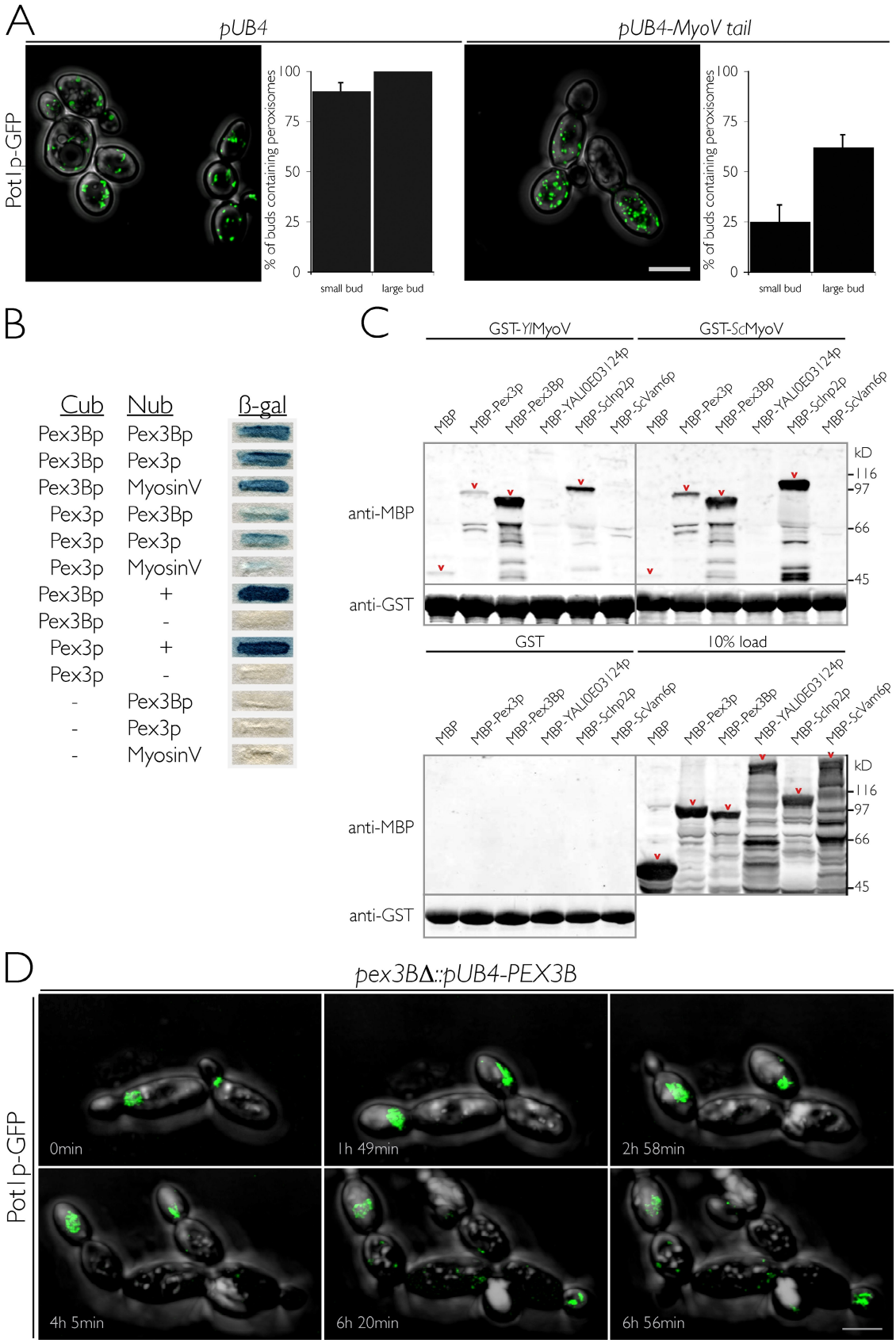

Figure 6. **Pex3Bp and Pex3p interact directly with the cargo-binding tail of *Y. lipolytica* class V myosin.** (A) Peroxisome inheritance is reduced by overexpression of the *Y. lipolytica* class V myosin cargo-binding tail. Wild-type strain *E122* expressing genomically encoded Pot1p-GFP to fluorescently label peroxisomes was transformed with the empty plasmid pUB4 or with pUB4 expressing the globular tail domain (amino acids 1,092–1,594) of *Y. lipolytica* class V myosin under the control of the oleic acid–inducible *POT1* promoter. Cells were grown in YPD supplemented with hygromycin B and then transferred

YPBO medium and imaged by confocal and electron microscopy (Fig. 8). Control strains containing empty plasmid presented the mutant phenotypes of *pex3Δ* and *pex3BΔ* cells; i.e., an absence of punctate peroxisomes and mislocalization of matrix proteins to the cytosol in *pex3Δ* cells and tubular-reticular peroxisomes, and compromised peroxisome inheritance in *pex3BΔ* cells (Fig. 8 A). Overexpression of Pex3Bp failed to complement the mutant phenotype of *pex3Δ* cells, whereas overexpression of Pex3p in either *pex3Δ* or *pex3BΔ* cells resulted in the appearance of large globular peroxisome clusters in addition to individual punctate peroxisomes (Fig. 8 A). Overexpression of Pex3Bp in *pex3BΔ* cells also resulted in the formation of globular peroxisome clusters, which were more compact than the clusters of *pex3BΔ* cells overexpressing Pex3p and were often located near the mother cell bud neck or in the bud itself (Fig. 8 A). That the large globular structures observed by fluorescence microscopy do in fact primarily represent clusters of small peroxisomes was confirmed by EM for *pex3BΔ* cells overexpressing *PEX3* or *PEX3B* (Fig. 8 B) and *pex3Δ* cells overexpressing *PEX3* (not depicted), as has been observed previously (Bascom et al., 2003). The *pex3BΔ* strain overexpressing *PEX3* also exhibited a peroxisome segregation phenotype (Fig. 8 A). Time-lapse 4D confocal microscopy of *pex3BΔ* cells containing fluorescently labeled peroxisomes and overexpressing *PEX3* showed that peroxisomes were preferentially transferred to daughter cells, leaving the mother cells without peroxisomes (Fig. 8 C and Video 5) Our data demonstrate that Pex3Bp overexpression in *pex3Δ* cells cannot reestablish the wild-type peroxisome phenotype. However, both Pex3p and Pex3Bp can function in the transfer of peroxisomes from mother cells to buds through a direct interaction with myosin V. Pex3p and Pex3Bp may also share some functions that remain undefined, namely with respect to their roles in regulating peroxisome morphology.

Discussion

Eukaryotic cells have evolved specific mechanisms for the faithful segregation of their organelles, including peroxisomes, during cell division. In general, organelle inheritance requires an expansion of the organelle population before cell division, retention of approximately half of the expanded organelle population by the mother cell, a cytoskeletal track for organelle movement from mother cell to daughter cell, a motor to carry the organelle along the cytoskeletal track, and an organelle-specific receptor that selectively recognizes the motor. Together, this highly orchestrated program permits the cell to temporally and spatially regulate the inheritance of one type of organelle from the inheritance of other types of organelle.

In *S. cerevisiae*, peroxisome inheritance relies on the actin cytoskeleton and is governed by the actions of two antagonistic proteins, Inp1p and Inp2p. Inp1p acts as a peroxisome-specific retention factor, tethering peroxisomes to putative anchoring structures within the mother cell and the bud (Fagarasanu et al., 2005), whereas Inp2p is the peroxisome-specific receptor for Myo2p (Fagarasanu et al., 2006), the class V myosin motor responsible for the directed traffic of most organelles from mother cell to bud in *S. cerevisiae* (Hoepfner et al., 2001).

As in *S. cerevisiae*, peroxisome movement and inheritance in *Y. lipolytica* are dependent on the actin cytoskeleton (Chang et al., 2007). *Y. lipolytica* also contains a homologue of Inp1p, which functions in peroxisome retention through its anchoring of peroxisomes to the cell cortex (Chang et al., 2007). Our interrogation of the *Y. lipolytica* genome revealed the presence of a single class V myosin gene in *Y. lipolytica* in contrast to the two class V myosin genes, *MYO2* and *MYO4*, in *S. cerevisiae*. Here we showed that the unique class V myosin of *Y. lipolytica* is required for the transfer of peroxisomes from mother cell to bud. However, interrogation of the *Y. lipolytica* genome revealed no strong candidate homologue of Inp2p, the peroxisome-specific myosin V receptor in *S. cerevisiae*. A putative Inp2p homologue, YALI0E03124p, was identified by iterative position-specific iterated BLAST analysis, but it was not shown to bind myosin V or to be localized to peroxisomes, two expected requirements for a peroxisome-specific receptor for myosin V. Nevertheless, the similarities in peroxisome inheritance between *S. cerevisiae* and *Y. lipolytica*, and our results showing that overexpression of the myosin V cargo-binding domain leads to reduced transfer of peroxisomes from mother cell to bud, led us to predict the presence of a peroxisome-specific receptor for the class V myosin of *Y. lipolytica*.

to and incubated in oleic acid–containing YPBO supplemented with hygromycin B for 6 h. Fluorescent images of randomly chosen fields of cells were acquired as a stack by confocal microscopy and then deconvolved. Buds were sized as "small" (0–39% of mother cell volume) or "large" (40–61% of mother cell volume; see Materials and methods). The percentages of buds containing peroxisomes in each size category are presented. Quantification was performed on at least 50 budded cells from each category. Graphic results are the means and SEM of three independent experiments. Bar, 5 μm. (B) Split-ubiquitin membrane yeast two-hybrid analysis. Cells of the *S. cerevisiae* strain *DSY-1* synthesizing Cub protein fusions to Pex3Bp or Pex3p and NubG protein fusions to Pex3Bp, Pex3p, or the globular tail of the class V myosin of *Y. lipolytica* (amino acids 1,092–1,594) were tested for their ability to interact with each other by a β-galactosidase filter detection assay. A positive interaction was detected by the production of blue color. The color intensities of positive (+) and negative (−) controls are indicated. (C) Glutathione sepharose beads containing GST fused to the cargo-binding tail of the class V myosin of *Y. lipolytica* (GST-YlMyoV); the cargo-binding tail of the class V myosin, Myo2p, of *S. cerevisiae* (GST-ScMyoV); or GST alone were incubated with extracts of *E. coli* synthesizing MBP, MBP-Pex3p, MBP-Pex3Bp, MBP-YALI0E03124p, MBP-ScInp2p, or MBP-ScVam6p. Bound proteins, as well as 10% of input proteins, were analyzed by immunoblotting with anti-MBP antibodies. Total GST-YlMyoV, GST-ScMyoV, or GST protein levels were visualized by immunoblotting with anti-GST antibodies. Arrowheads indicate MBP or MBP fusion proteins. (D) Overexpression of *PEX3B* delivers peroxisomes preferentially to buds. *pex3BΔ* cells containing peroxisomes labeled with Pot1p-GFP and the plasmid pUB4 expressing *PEX3B* under the control of the oleic acid–inducible *POT1* promoter were grown for 16 h in YPD supplemented with hygromycin B, then transferred to oleic acid–containing YPBO supplemented with hygromycin B for 6 h, and visualized at 23°C with an LSM 510 confocal microscope specifically modified for 4D in vivo microscopy (see Materials and methods). Representative frames from Video 4 show the specific movements of peroxisomes and their inheritance from mother cell to bud. At 0 min, two large peroxisome clusters are initially located next to the mother-bud neck. By 1 h 49 min, these peroxisomes have been transferred to their respective buds, and by 4 h 5 min, the cycle is repeated, with the peroxisomes now residing in the granddaughters of the original mother cells. De novo synthesis of peroxisomes can also be detected by the reappearance of fluorescent punctae in mother cells that had transferred their original peroxisome complement to their buds. These de novo formed peroxisomes are also vectorially transferred to newly formed buds (6 h 20 min). The formation of peroxisomes and subsequent transfer to buds continued (6 h 56 min). Bar, 5 μm.

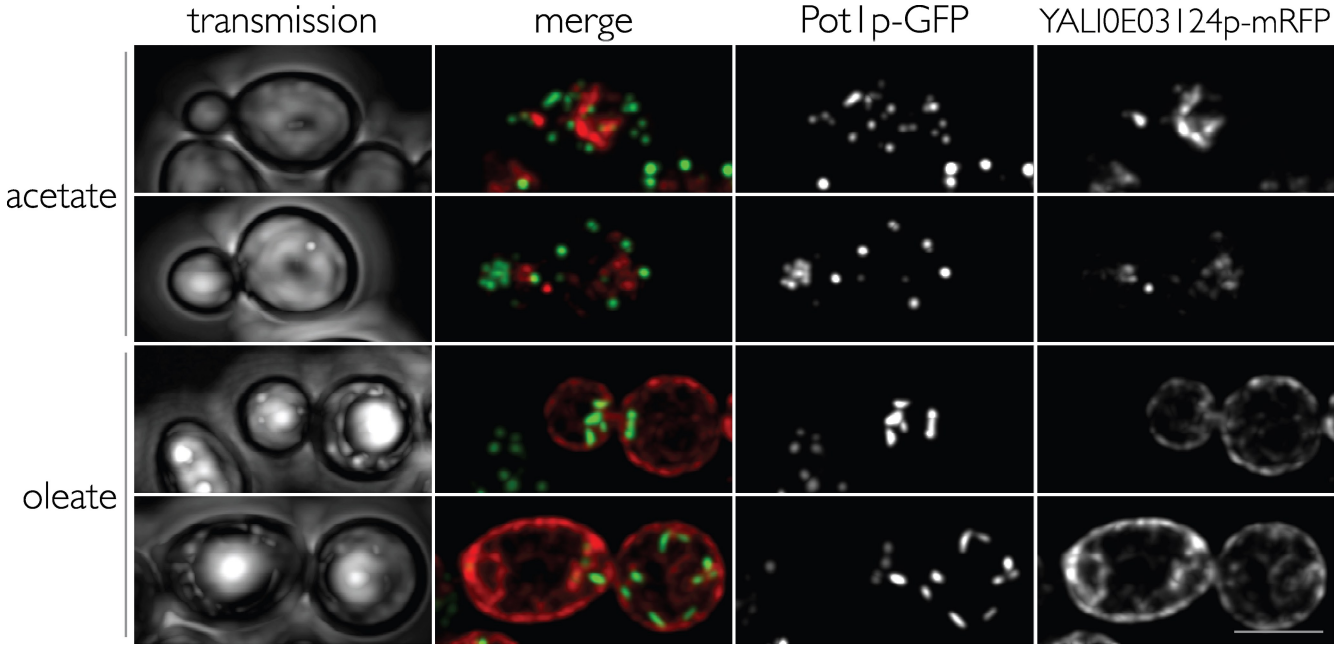

Figure 7. **A candidate *Y. lipolytica* Inp2p orthologue, YALI0E03124p, does not localize to peroxisomes**. The chimeric protein YALI0E03124p-mRFP, whose expression is under the control of the oleic acid–inducible promoter *POT1*, was imaged in the wild-type strain *E122* expressing genomically integrated Pot1p-GFP to fluorescently label peroxisomes. YALI0E03124p-mRFP did not localize to punctate peroxisomes, and when cells were incubated in oleic acid–containing medium, YALI0E03124p-mRFP exhibited a pattern typical of protein localization to the ER and secretory system. The top panels show representative images of cells grown in medium containing acetate, whereas the bottom panels show representative images of cells grown in medium containing oleic acid. Bar, 5 µm.

Surprisingly, we found that the early acting peroxisome biogenesis protein, Pex3p, and its paralogue Pex3Bp, function as peroxisome-specific receptors for the class V myosin of *Y. lipolytica*. Several lines of evidence support this conclusion: (1) Pex3p and Pex3Bp are integral membrane proteins of peroxisomes, fulfilling the spatial specificity requirement for a peroxisome-specific receptor. (2) Deletion of the *PEX3B* gene results in the inability of cells to properly segregate peroxisomes, leaving many buds devoid of peroxisomes, a phenotype observed in *S. cerevisiae* cells lacking *INP2* (Fagarasanu et al., 2006). Also, the lack of saltatory, vectorial movements of peroxisomes seen in *pex3BΔ* cells is consistent with an uncoupling of peroxisomes from the myosin V motor. (3) Pex3p and Pex3Bp interact directly with myosin V, thus satisfying the requirement for a direct connection between the motor and its organelle receptor. Interestingly, we also detected an interaction between Pex3p or Pex3Bp and Myo2p, the myosin V motor protein that transports peroxisomes in *S. cerevisiae*. Likewise, Inp2p was found to bind the myosin V of *Y. lipolytica* (Fig. 6 C). These interactions are consistent with the idea that conserved patches on the surfaces of cargo-binding domains of myosin Vs from different organisms serve to bind specific cargoes (Pashkova et al., 2006). It is tempting to speculate that there exists a conserved interorganismal patch for peroxisome receptors on the surface of class V myosin tails. (4) Overexpression of Pex3p or Pex3Bp leads to preferential partitioning of peroxisomes to buds, leaving many mother cells without peroxisomes. Likewise, overexpression of Inp2p also leads to the concentration of the peroxisome population in buds and increased numbers of mother cells without peroxisomes (Fagarasanu et al., 2006). (5) The failure to correctly segregate peroxisomes in cells either lacking or overexpressing Pex3Bp activates de novo peroxisome biogenesis in the empty buds and mother cells, respectively (Videos 2 and 4). This is similar to what is observed in mutants of vacuole inheritance in which buds without vacuoles are rapidly able to form new vacuolar structures de novo, thereby allowing the bud to develop and go on to produce daughter cells of its own (Weisman et al., 1987; Raymond et al., 1990; Gomes De Mesquita et al., 1997).

Although the overall process of peroxisome inheritance is similar in *S. cerevisiae* and *Y. lipolytica*, there are differences. First, the localization of Pex3p (Bascom et al., 2003) or Pex3Bp to peroxisomes is not polarized; i.e., it is not preferentially associated with those peroxisomes that are inherited, as is the case for Inp2p (Fagarasanu et al., 2006). This might suggest that it is not the levels of Pex3p or Pex3Bp that dictate the segregation fate of peroxisomes but rather that Pex3p or Pex3Bp could be activated via a posttranslational modification, such as phosphorylation, which would enable it to engage the class V myosin motor. *S. cerevisiae* Vac17p, the vacuole-specific receptor for Myo2p, has been shown to be phosphorylated at multiple sites, which is important both for its activation and its targeting to degradation (Peng and Weisman, 2008; Bartholomew and Hardy, 2009). We also cannot exclude the presence of a regulatory protein that governs the interaction between Pex3p or Pex3Bp and myosin V. A requirement for additional regulatory subunits in the receptor–myosin transport complex has been postulated previously (Ishikawa et al., 2003; Weisman, 2006).

Interestingly, both Inp2p and Vac17p in *S. cerevisiae* function exclusively as the adaptor molecules for Myo2p on peroxisomes and vacuoles, respectively, without apparently performing any other metabolic or biogenic function in their respective organelles (Ishikawa et al., 2003; Fagarasanu et al., 2006). This

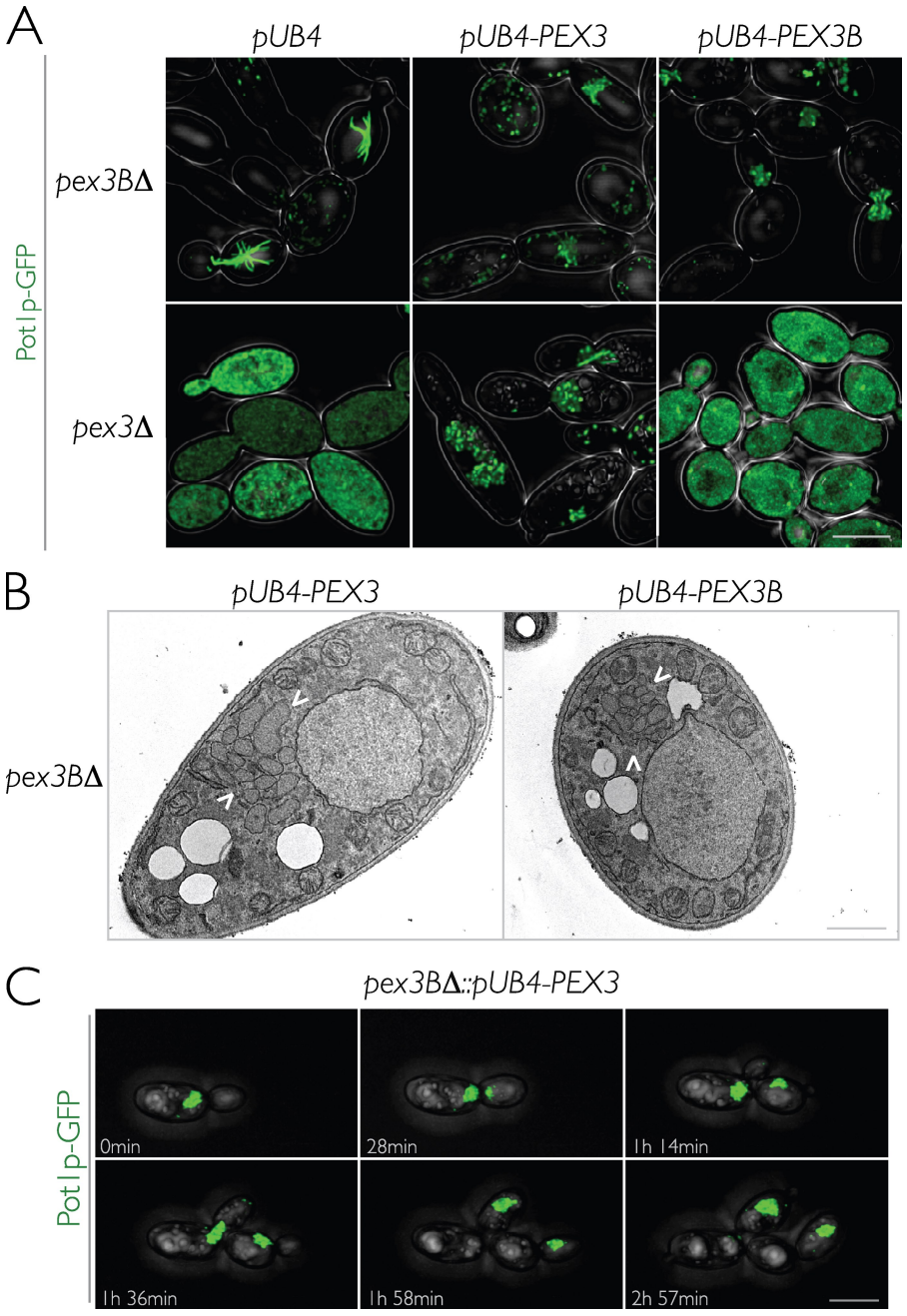

Figure 8. **Pex3p can substitute for Pex3Bp in peroxisome inheritance.** (A) *pex3BΔ* and *pex3Δ* cells expressing genomically integrated Pot1p-GFP were transformed with empty plasmid pUB4 or pUB4 containing *PEX3B* or *PEX3* for overexpression in oleic acid–containing medium. Cells were grown in YPD supplemented with hygromycin B and then transferred and incubated for 6 h in oleic acid–containing YPBO supplemented with hygromycin B. Fluorescent images of cells were captured by confocal microscopy and deconvolved. Bar, 5 µm. (B) Ultrastructure of *pex3BΔ* cells overexpressing *PEX3B* or *PEX3*. Cells were cultured as in A and then fixed and processed for EM. Arrowheads indicate peroxisomes. Bar, 1 µm. (C) Overexpression of *PEX3* can rescue the *pex3BΔ* phenotype. *pex3BΔ* cells containing peroxisomes labeled with Pot1p-GFP and the plasmid pUB4 expressing *PEX3* under the control of the oleic acid–inducible *POT1* promoter were grown and imaged as in Fig. 6 D (see Materials and methods). Representative frames from Video 5 show the specific movements of peroxisomes and their inheritance from mother cell to bud. At 0 min, one large peroxisome cluster is initially located near the mother-bud neck. By 28 min, the peroxisome cluster is split in two by cytokinesis. As new buds emerge, these peroxisome clusters are transferred to the new buds. Several single peroxisomes can be seen at the bud tip by 1 h 36 min. As the buds continue to grow, the peroxisome clusters also move to the bud tips. Bar, 5 µm.

has led to the view that organelle-specific receptors for myosins are devoted solely to organelle motility and are thus able to fluctuate during the cell cycle without altering the metabolic efficiency of organelles (Fagarasanu et al., 2007). However, this view has recently been challenged by the discovery of Ypt31p/Ypt32p as the receptor for post-Golgi secretory vesicles (Lipatova et al., 2008). The Ypt31p/Ypt32p GTPase functional pair plays a major role in the budding of trans-Golgi–derived vesicles. Its other role in recruiting Myo2p to vesicle membranes therefore links temporally the biogenesis of secretory vesicles with their bud-destined transport. Similarly, members of the Pex3p family appear to be multifunctional, having roles in de novo peroxisome biogenesis and in regulating peroxisome morphology and inheritance.

With the demonstration of a role for the Pex3 protein family in peroxisome inheritance, several exciting possibilities arise. For example, it is tempting to speculate that Pex3 proteins are part of a mechanism that ensures the preferential transfer of new peroxisomal material to daughter cells. If Pex3 proteins are involved in both the production of peroxisomes at the ER and the recruitment of myosin to their membranes, the newly formed peroxisomal vesicles would probably be admirably equipped to harness the robust anterograde-directed machinery to promote their transfer to the bud. Therefore, we may have unraveled a mechanism that relates the age of peroxisomes with their segregation fates. Importantly, through their specific metabolic functions, peroxisomes are exposed to potentially damaging reactive oxygen species (Smith and Aitchison, 2009). It is well accepted that oxidized proteins are

important factors in replicative aging (Macara and Mili, 2008). The proposed model wherein newer peroxisomal material is preferentially inherited by the daughter cell would predict that oxidatively damaged peroxisomal proteins accumulate in the mother cell, explaining in part how deleterious material is differentially retained by the aging cell. Because the Pex3 family of proteins is highly conserved throughout the eukaryotes, the temporal connection between peroxisome biogenesis and their motility might be a common mechanism in peroxisome inheritance. Notably, it has previously been observed that overproduction of Pex3p in *S. cerevisiae* cells leads to the transfer of all peroxisomes to the growing bud (Tam et al., 2005). However, deletion of the *PEX3* gene in any organism studied so far has led to a complete loss of peroxisomes, and therefore the presence of two members of the Pex3 protein family in *Y. lipolytica* may have offered an "evolutionary" window of opportunity for the direct observation of an as of yet unknown contribution of Pex3 proteins to peroxisome motility.

Although our findings readily show that the Pex3 protein family is involved in peroxisome inheritance, we have not resolved the cellular mechanisms that lead to the observed imbalance of peroxisome division in Pex3Bp deletion and Pex3p/Pex3Bp overexpression strains. Elongation of peroxisomes in cells lacking Pex3Bp might be caused indirectly by the inefficiency of the association of myosin V with the peroxisomal membrane. Cytoskeletal tracks and motor proteins are known to exert tensions on organelle membranes, thus assisting in organelle fission (Schrader and Fahimi, 2008). It has been suggested previously that the pulling forces exerted by the machinery that propels the bud-directed movement of peroxisomes on the one hand and peroxisome retention mechanisms on the other act on the membranes of peroxisomes to sever them (Fagarasanu et al., 2007; Motley and Hettema, 2007). The clustering of peroxisomes seen in cells overexpressing Pex3Bp or Pex3p might be explained by our two-hybrid data, which showed that Pex3Bp and Pex3p can interact with themselves and with each other. This would allow peroxisomes to associate with one another via protein interactions in trans. Further studies are needed to determine how the interactions between Pex3p, Pex3Bp, and myosin V function in the recruitment of division and/or other inheritance factors to the peroxisomal membrane and whether these interactions contribute to the overall morphology of peroxisomes. These studies would also help to elucidate how peroxisome biogenesis, division, and inheritance are linked.

In closing, we have demonstrated an unexpected role for the early acting Pex3 peroxisome biogenesis proteins in peroxisome inheritance and motility through their direct coupling of peroxisomes to the myosin V motor protein. Our studies reveal a general mechanism of peroxisome inheritance and point to a temporal link between peroxisome formation and inheritance mediated through the Pex3 proteins.

Materials and methods

Strains and culture conditions

The *Y. lipolytica* strains used in this study are listed in Table S1. Strains were cultured at 30°C unless otherwise indicated. Strains containing plasmid pUB4 were cultured in YPD or YPBO supplemented with hygromycin B at 125 µg/ml. Strains containing plasmid pTC3 were cultured in YNA or YNO medium supplemented with lysine at 50 µg/ml. Media components were as follows: YPD, 1% yeast extract, 2% peptone, and 2% glucose; YPBO, 0.3% yeast extract, 0.5% peptone, 1% Brij 35, 1% [vol/vol] oleic acid, 0.5% K_2HPO_4, and 0.5% KH_2PO_4; YNO, 1.34% yeast nitrogen base without amino acids, 0.05% [wt/vol] Tween 40, 0.2% [wt/vol] oleic acid; and YNA, 1.34% yeast nitrogen base without amino acids and 2% sodium acetate.

Integrative transformation of yeast

The *PEX3B* gene was disrupted and the *POT1* gene was tagged with a sequence coding for GFP by homologous transformation of yeast using a fusion PCR-based integrative procedure (Davidson et al., 2002).

Plasmids

The plasmids pTC3 (Lin et al., 1999) and pUB4 (Kerscher et al., 2001) have been described previously. The chimeric genes *PEX3B-mRFP* and *YALI0E03124g-mRFP* were made by fusion PCR (Davidson et al., 2002) and inserted at the EcoRI site of pTC3 to make the expression plasmid pTC3-PEX3B-mRFP and pTC3-YALI0E03124g-mRFP, respectively. *PEX3B-mRFP* flanked by the promoter and terminator regions of the *POT1* gene encoding peroxisomal thiolase was amplified by PCR of pTC3-PEX3B-mRFP and inserted into the ClaI site of pUB4 to make the plasmid pUB4-PEX3B-mRFP. The genes *MYOV*, *PEX3B*, and *PEX3* were inserted into pTC3 and amplified individually with the promoter and terminator regions of *POT1* by PCR as described for pUB4-PEX3B-mRFP to make the plasmids pUB4-MyoVtail, pUB4-PEX3B, and pUB4-PEX3.

Staining of cell structures

Actin, vacuoles, and mitochondria were stained with rhodamine-phalloidin, *N*-(3-triethylammoniumpropyl)-(6(4(diethylamino)phenyl)hexatrienyl)pyridium dibromide (FM 4–64), and MitoTracker Red CMXRos, respectively (all from Invitrogen).

Microscopy

Fluorescent images were captured with a Plan-Apochromat 63×/1.4 numerical aperture oil differential interference contrast objective lens on an Axiovert 200 microscope equipped with a LSM510 META confocal scanner (Carl Zeiss, Inc.). EM of whole yeast cells was performed using standard techniques (Eitzen et al., 1997).

4D in vivo microscopy

Cells synthesizing a genomically encoded chimera between Pot1p and GFP (Pot1p-GFP) were cultured as described in the legends to Figs. 5, 6 D, and 8 C. 4D in vivo video microscopy was performed on an Axiovert 200 microscope equipped with an LSM 510 META confocal scanner (Fagarasanu et al., 2006). For Fig. 5 (A and B) and Videos 1 and 2, cells were placed in a 35-mm Petri dish with a 14-mm microwell No. 1.5 borosilicate coverglass (MatTek) and incubated at a constant temperature of 28°C in a microscope stage and cage dual-incubator system controlled by Read-Temperature software (Okolab). Images were captured with an LCI Plan-Neofluar 63×/1.3 numerical aperture multi-immersion differential interference contrast objective with an adjustable correction collar (Carl Zeiss, Inc.). For Figs. 5 C, 6 D, and 8 C; and Videos 3, 4, and 5, cells were placed in a chambered No. 1.0 borosilicate coverglass (Lab-Tek; Thermo Fisher Scientific) coated with concanavalin A and incubated at 23°C for image capture with a Plan-Apochromat 63×/1.4 numerical aperture oil differential interference contrast objective (Carl Zeiss, Inc.). A piezoelectric actuator was used to drive continuous objective movement, allowing for the rapid collection of z stacks (Hammond and Glick, 2000). The sides of each pixel represent 0.09 µm of the sample. Stacks of 30 optical sections spaced 0.3 µm apart were captured every 60 s. GFP was excited using a 488-nm laser, and its emission was collected using a 505-nm long-pass filter.

Deconvolution and image manipulation

To remove blur, experimentally generated 3D and 4D datasets were deconvolved through an iterative classical maximum likelihood estimation algorithm and an experimentally derived point spread function using Huygens Professional software (Scientific Volume Imaging BV). Imaris software (Bitplane) was subsequently used to prepare maximum intensity projections or "Blend-view" projections of the deconvolved 3D and 4D datasets. These projections were used to generate single images or videos. The collections of images were then assembled into figures using Photoshop CS3 and InDesign CS3 (Adobe). The transmission images with labeled mitochondria or vacuoles in Fig. 4 B were altered to display only the cell border, thereby allowing better visualization, but no alteration, of data from the fluorescent channels. The "Circular Marquee" tool in Photoshop CS3 was used to select data from the transmission channel and delete them from the images.

In Fig. 3 D, peroxisomes were outlined for better visualization using the "Pencil" tool in Photoshop CS3.

Quantification of rates of peroxisome inheritance

Rates of peroxisome inheritance were quantified as described previously (Fagarasanu et al., 2006). Essentially, cells expressing Pot1p-GFP were grown in YPD medium for 16 h and then transferred to and incubated in YPBO medium for 2 h (Fig. 4) or 6 h (Fig. 6). Peroxisomes were visualized by direct fluorescence confocal microscopy. For each randomly chosen field, three optical sections of 5 µm thickness each were collected at a z axis spacing of 1.6 µm using a high detector gain to ensure the capture of weak fluorescent signals. Optical sections were then projected onto a single image. All visibly budded cells were considered for analysis, and buds were assigned to four categories of bud volume, expressed as a percentage of mother cell volume (category I, 0–12%; category II, 13–24%; category III, 25–36%; category IV, 37–48%). Because cell volume is not directly accessible, bud area was first measured using LSM510 Image Browser software (Carl Zeiss, Inc.) and grouped into four "area" categories, which superimpose on the aforementioned "volume" categories if a spherical geometry is assumed for all cells, according to the bud cross-sectional area expressed as a percentage of mother cell cross-sectional area (category I, 0–24%; category II, 25–39%; category III, 40–50%; category IV, 50–61%). Bud tips were then scored using an all-or-none criterion for the presence or absence of peroxisomal fluorescence. To measure the efficiency of peroxisome inheritance in cells expressing the globular tail domain of the type V myosin of *Y. lipolytica*, budded cells were assigned to two size categories: "small budded cells" representing the merger of categories I and II and "large budded cells" representing the merger of categories III and IV.

Cell fractionation and organelle extraction

Wild-type cells transformed with pUB4-PEX3B-mRFP were cultured in YPD medium supplemented with hygromycin B at 125 µg/ml. Cell fractionation was performed essentially as described previously (Szilard et al., 1995). Homogenized spheroplasts were subjected to differential centrifugation at 1,000 *g* for 10 min at 4°C in a JS13.1 rotor (Beckman Coulter) to yield a postnuclear supernatant (PNS) fraction. The PNS fraction was subjected to further differential centrifugation at 20,000 *g* for 30 min at 4°C to yield a pellet (20KgP) fraction enriched for peroxisomes and a supernatant (20KgS) fraction enriched for cytosol. The 20KgP fraction was separated into fractions enriched for matrix, peripheral, and integral membrane proteins by treatment with dilute Tris and alkali Na_2CO_3 as described previously (Vizeacoumar et al., 2003).

Isolation of peroxisomes

Wild-type cells were induced in YPBO, and the 20KgP was prepared as described in "Cell fractionation and organelle extraction." Peroxisomes were purified from the 20KgP fraction by isopycnic centrifugation on a discontinuous sucrose gradient (Titorenko et al., 1996).

Split-ubiquitin membrane yeast two-hybrid analysis

Physical interactions between Pex3Bp, Pex3p, and the globular tail (amino acids 1,092–1,594) of the class V myosin of *Y. lipolytica* were detected using the split-ubiquitin membrane yeast two-hybrid system (Dualsystems Biotech AG; Stagljar et al., 1998). Bait vectors were constructed by amplifying the sequences of target genes by PCR and ligating them into the plasmid vector pTMBV4 in-frame and upstream of the C-terminal half of ubiquitin (Cub) and the chimeric transcriptional reporter LexA-VP-16 to make the construct gene-Cub-LexA-VP-16. Prey vectors were constructed by ligating target genes into the vector plasmid pADL-xN in-frame and upstream of the N-terminal half of ubiquitin (NubG) to make the construct gene-NubG. *S. cerevisiae* strain *DSY-1* was transformed with both bait and prey plasmids. Transformants were grown on synthetic medium (SM) agar lacking the amino acids leucine (auxotrophic selection marker for the bait vector pTMBV4) and tryptophan (auxotrophic selection marker for the prey vector pADL-xN). Interaction between bait and prey was shown by expression of *HIS3* and growth on SM agar lacking histidine and by activation of the *LacZ* reporter gene and production of blue color from a chromogenic substrate in a β-galactosidase filter assay.

Assay for direct protein binding

A GST fusion protein of the globular tail (amino acids 1,092–1,594) of the class V myosin of *Y. lipolytica* (GST-YlMyoV) was constructed using pGEX4T-1 (GE Healthcare). The fusion between GST and the class V myosin Myo2p of *S. cerevisiae* (GST-ScMyoV; Fagarasanu et al., 2006) was a kind gift from A. Fagarasanu (University of Alberta, Edmonton, Alberta, Canada). Recombinant expression and immobilization of GST, GST-YlMyoV, and GST-ScMyoV were done according to the manufacturer's instructions. MBP fusions to Pex3p, Pex3Bp, YALI0E03124p, and ScVam6p were made using pMAL-c2 (New England Biolabs, Inc.) and expressed in the *E. coli* strain BL21 (Invitrogen). MBP-ScInp2p has been described previously (Fagarasanu et al., 2006).

250 µg of purified GST, GST-ScMyoV, or GST-YlMyoV protein immobilized on glutathione resin was incubated with 250 µg of *E. coli* lysate containing an MBP fusion or MBP alone in H buffer (20 mM Hepes, pH 7.4, 120 mM NaCl, 5 mM $MgCl_2$, 0.5 mM dithiothreitol, 0.5% [vol/vol] Triton X-100, and 1× complete protease inhibitors [Roche]) for 3 h at 4°C on a rocking platform. The immobilized fractions were allowed to settle and were then washed five times with H buffer and eluted in sample buffer (50 mM Tris-HCl, pH 6.8, 2% SDS, 5% [vol/vol] glycerol, 0.001% bromophenol blue, and 5% [vol/vol] 2-mercaptoethanol). The eluted proteins were subjected to SDS-PAGE and immunoblotting.

Antibodies

Antibodies to Pex3Bp were raised in guinea pigs against a GST/Pex3Bp fusion. The ORF of *PEX3B* was amplified by PCR and cloned into the plasmid pGEX4T-1 downstream and in-frame to the ORF for GST, followed by expression in *E. coli*. Antibodies to Sdh2p, Pex2p, and Pot1p have been described previously (Eitzen et al., 1996; Fagarasanu et al., 2005). Rabbit anti-DsRed polyclonal antibody was obtained from Takara Bio, Inc. For routine immunoblot analysis, horseradish peroxidase–conjugated donkey anti–rabbit IgG and horseradish peroxidase–conjugated goat anti–guinea pig IgG secondary antibodies were used to detect primary antibodies, and antigen–antibody complexes were detected by enhanced chemiluminescence (GE Healthcare). Immunoblotting with rabbit antibodies to MBP (New England Biolabs, Inc.) and mouse monoclonal antibodies to GST (Sigma-Aldrich), combined with Alexa Fluor 680/750–conjugated goat anti–mouse/anti–rabbit antibodies (Invitrogen), was used to detect protein interactions in the assay for direct protein binding. Immunoblots were processed using an Odyssey digital imaging system (LI-COR Biosciences) with resolution set at 84 µm and at the highest quality.

Online supplemental material

Fig. S1 shows that Pex3Bp cofractionates with the peroxisomal marker thiolase but not with the mitochondrial marker Sdh2 on a sucrose gradient subjected to isopycnic centrifugation. Video 1 shows peroxisome dynamics during wild-type cell division. Videos 2 and 3 show peroxisome dynamics during cell division in *pex3BΔ* mutants. Video 4 shows peroxisome dynamics during cell division in cells overexpressing PEX3B. Video 5 shows peroxisome dynamics during cell division in cells overexpressing PEX3. Table S1 lists yeast strains used in this study and their genotypes. Online supplemental material is available at http://www.jcb.org/cgi/content/full/jcb.200902117/DC1.

We thank Richard Poirier, Hanna Kroliczak, David Lancaster, Elena Savidov, Dwayne Weber, and Honey Chan for expert technical assistance and members of the Rachubinski laboratory for helpful discussions.

J. Chang was supported by a Queen Elizabeth II Graduate Scholarship. F.D. Mast was supported by a Canada Graduate Scholarship from the Canadian Institutes of Health Research (CIHR) and a Faculty of Medicine & Dentistry 75th Anniversary Award. R.A. Rachubinski is an International Research Scholar of the Howard Hughes Medical Institute. This work was supported by operating grant 9208 from the CIHR to R.A. Rachubinski.

Submitted: 23 February 2009
Accepted: 11 September 2009

References

Altschul, S.F., T.L. Madden, A.A. Schäffer, J. Zhang, Z. Zhang, W. Miller, and D.J. Lipman. 1997. Gapped BLAST and PSI-BLAST: a new generation of protein database search programs. *Nucleic Acids Res.* 25:3389–3402. doi:10.1093/nar/25.17.3389.

Bartholomew, C.R., and C.F.J. Hardy. 2009. p21-activated kinases Cla4 and Ste20 regulate vacuole inheritance in *Saccharomyces cerevisiae*. *Eukaryot. Cell.* 8:560–572.

Bascom, R.A., H. Chan, and R.A. Rachubinski. 2003. Peroxisome biogenesis occurs in an unsynchronized manner in close association with the endoplasmic reticulum in temperature-sensitive *Yarrowia lipolytica* Pex3p mutants. *Mol. Biol. Cell.* 14:939–957. doi:10.1091/mbc.E02-10-0633.

Chang, J., A. Fagarasanu, and R.A. Rachubinski. 2007. Peroxisomal peripheral membrane protein YlInp1p is required for peroxisome inheritance and influences the dimorphic transition in the yeast *Yarrowia lipolytica*. *Eukaryot. Cell.* 6:1528–1537.

Davidson, R.C., J.R. Blankenship, P.R. Kraus, M. de Jesus Berrios, C.M. Hull, C. D'Souza, P. Wang, and J. Heitman. 2002. A PCR-based strategy to generate integrative targeting alleles with large regions of homology. *Microbiology.* 148:2607–2615.

Eitzen, G.A., V.I. Titorenko, J.J. Smith, M. Veenhuis, R.K. Szilard, and R.A. Rachubinski. 1996. The *Yarrowia lipolytica* gene *PAY5* encodes a peroxisomal integral membrane protein homologous to the mammalian peroxisome assembly factor PAF-1. *J. Biol. Chem.* 271:20300–20306. doi:10.1074/jbc.271.34.20307.

Eitzen, G.A., R.K. Szilard, and R.A. Rachubinski. 1997. Enlarged peroxisomes are present in oleic acid-grown *Yarrowia lipolytica* overexpressing the *PEX16* gene encoding an intraperoxisomal peripheral membrane peroxin. *J. Cell Biol.* 137:1265–1278. doi:10.1083/jcb.137.6.1265.

Erdmann, R., and G. Blobel. 1995. Giant peroxisomes in oleic acid-induced *Saccharomyces cerevisiae* lacking the peroxisomal membrane protein Pmp27p. *J. Cell Biol.* 128:509–523. doi:10.1083/jcb.128.4.509.

Fagarasanu, M., A. Fagarasanu, Y.Y.C. Tam, J.D. Aitchison, and R.A. Rachubinski. 2005. Inp1p is a peroxisomal membrane protein required for peroxisome inheritance in *Saccharomyces cerevisiae. J. Cell Biol.* 169:765–775. doi:10.1083/jcb.200503083.

Fagarasanu, A., M. Fagarasanu, G.A. Eitzen, J.D. Aitchison, and R.A. Rachubinski. 2006. The peroxisomal membrane protein Inp2p is the peroxisome-specific receptor for the myosin V motor Myo2p of *Saccharomyces cerevisiae. Dev. Cell.* 10:587–600. doi:10.1016/j.devcel.2006.04.012.

Fagarasanu, A., M. Fagarasanu, and R.A. Rachubinski. 2007. Maintaining peroxisome populations: a story of division and inheritance. *Annu. Rev. Cell Dev. Biol.* 23:321–344. doi:10.1146/annurev.cellbio.23.090506.123456.

Fujiki, Y., A.L. Hubbard, S. Fowler, and P.B. Lazarow. 1982. Isolation of intracellular membranes by means of sodium carbonate treatment: application to endoplasmic reticulum. *J. Cell Biol.* 93:97–102. doi:10.1083/jcb.93.1.97.

Fujiki, Y., Y. Matsuzono, T. Matsuzaki, and M. Fransen. 2006. Import of peroxisomal membrane proteins: the interplay of Pex3p- and Pex19p-mediated interactions. *Biochim. Biophys. Acta.* 1763:1639–1646. doi:10.1016/j.bbamcr.2006.09.030.

Geuze, H.J., J.L. Murk, A.K. Stroobants, J.M. Griffith, M.J. Kleijmeer, A.J. Koster, A.J. Verkleij, B. Distel, and H.F. Tabak. 2003. Involvement of the endoplasmic reticulum in peroxisome formation. *Mol. Biol. Cell.* 14:2900–2907. doi:10.1091/mbc.E02-11-0734.

Gomes De Mesquita, D.S., J. Shaw, J.A. Grimbergen, M.A. Buys, L. Dewi, and C.L. Woldringh. 1997. Vacuole segregation in the *Saccharomyces cerevisiae vac2-1* mutant: structural and biochemical quantification of the segregation defect and formation of new vacuoles. *Yeast.* 13:999–1008. doi:10.1002/(SICI)1097-0061(19970915)13:11<999::AID-YEA151>3.0.CO;2-0.

Hammond, A.T., and B.S. Glick. 2000. Raising the speed limits for 4D fluorescence microscopy. *Traffic.* 1:935–940. doi:10.1034/j.1600-0854.2000.011203.x.

Hoepfner, D., M. van den Berg, P. Philippsen, H.F. Tabak, and E.H. Hettema. 2001. A role for Vps1p, actin, and the Myo2p motor in peroxisome abundance and inheritance in *Saccharomyces cerevisiae. J. Cell Biol.* 155:979–990. doi:10.1083/jcb.200107028.

Hoepfner, D., D. Schildknegt, I. Braakman, P. Philippsen, and H.F. Tabak. 2005. Contribution of the endoplasmic reticulum to peroxisome formation. *Cell.* 122:85–95. doi:10.1016/j.cell.2005.04.025.

Ishikawa, K., N.L. Catlett, J.L. Novak, F. Tang, J.J. Nau, and L.S. Weisman. 2003. Identification of an organelle-specific myosin V receptor. *J. Cell Biol.* 160:887–897. doi:10.1083/jcb.200210139.

Kerscher, S.J., A. Eschemann, P.M. Okun, and U. Brandt. 2001. External alternative NADH:ubiquinone oxidoreductase redirected to the internal face of the mitochondrial inner membrane rescues complex I deficiency in *Yarrowia lipolytica. J. Cell Sci.* 114:3915–3921.

Kiel, J.A.K.W., M. Veenhuis, and I.J. van der Klei. 2006. *PEX* genes in fungal genomes: common, rare or redundant. *Traffic.* 7:1291–1303. doi:10.1111/j.1600-0854.2006.00479.x.

Lazarow, P.B. 2003. Peroxisome biogenesis: advances and conundrums. *Curr. Opin. Cell Biol.* 15:489–497. doi:10.1016/S0955-0674(03)00082-6.

Lazarow, P.B., and Y. Fujiki. 1985. Biogenesis of peroxisomes. *Annu. Rev. Cell Biol.* 1:489–530. doi:10.1146/annurev.cb.01.110185.002421.

Lin, Y., L. Sun, L.V. Nguyen, R.A. Rachubinski, and H.M. Goodman. 1999. The Pex16p homolog SSE1 and storage organelle formation in *Arabidopsis* seeds. *Science.* 284:328–330. doi:10.1126/science.284.5412.328.

Lipatova, Z., A.A. Tokarev, Y. Jin, J. Mulholland, L.S. Weisman, and N. Segev. 2008. Direct interaction between a myosin V motor and the Rab GTPases Ypt31/32 is required for polarized secretion. *Mol. Biol. Cell.* 19:4177–4187. doi:10.1091/mbc.E08-02-0220.

Macara, I.G., and S. Mili. 2008. Polarity and differential inheritance—universal attributes of life? *Cell.* 135:801–812. doi:10.1016/j.cell.2008.11.006.

Motley, A.M., and E.H. Hettema. 2007. Yeast peroxisomes multiply by growth and division. *J. Cell Biol.* 178:399–410. doi:10.1083/jcb.200702167.

Novikoff, P.M., and A.B. Novikoff. 1972. Peroxisomes in absorptive cells of mammalian small intestine. *J. Cell Biol.* 53:532–560. doi:10.1083/jcb.53.2.532.

Novikoff, A.B., and W.-Y. Shin. 1964. The endoplasmic reticulum in the Golgi zone and its relations to microbodies, Golgi apparatus and autophagic vacuoles in rat liver cells. *J. Microsc.* 3:187–206.

Pashkova, N., Y. Jin, S. Ramaswamy, and L.S. Weisman. 2006. Structural basis for myosin V discrimination between distinct cargoes. *EMBO J.* 25:693–700. doi:10.1038/sj.emboj.7600965.

Peng, Y., and L.S. Weisman. 2008. The cyclin-dependent kinase Cdk1 directly regulates vacuole inheritance. *Dev. Cell.* 15:478–485. doi:10.1016/j.devcel.2008.07.007.

Raymond, C.K., P.J. O'Hara, G. Eichinger, J.H. Rothman, and T.H. Stevens. 1990. Molecular analysis of the yeast *VPS3* gene and the role of its product in vacuolar protein sorting and vacuolar segregation during the cell cycle. *J. Cell Biol.* 111:877–892. doi:10.1083/jcb.111.3.877.

Schrader, M., and H.D. Fahimi. 2008. The peroxisome: still a mysterious organelle. *Histochem. Cell Biol.* 129:421–440. doi:10.1007/s00418-008-0396-9.

Smith, J.J., and J.D. Aitchison. 2009. Regulation of peroxisome dynamics. *Curr. Opin. Cell Biol.* 21:119–126. doi:10.1016/j.ceb.2009.01.009.

Stagljar, I., C. Korostensky, N. Johnsson, and S. te Heesen. 1998. A genetic system based on split-ubiquitin for the analysis of interactions between membrane proteins *in vivo. Proc. Natl. Acad. Sci. USA.* 95:5187–5192. doi:10.1073/pnas.95.9.5187.

Steinberg, S.J., G. Dodt, G.V. Raymond, N.E. Braverman, A.B. Moser, and H.W. Moser. 2006. Peroxisome biogenesis disorders. *Biochim. Biophys. Acta.* 1763:1733–1748. doi:10.1016/j.bbamcr.2006.09.010.

Szilard, R.K., V.I. Titorenko, M. Veenhuis, and R.A. Rachubinski. 1995. Pay32p of the yeast *Yarrowia lipolytica* is an intraperoxisomal component of the matrix protein translocation machinery. *J. Cell Biol.* 131:1453–1469. doi:10.1083/jcb.131.6.1453.

Tam, Y.Y.C., A. Fagarasanu, M. Fagarasanu, and R.A. Rachubinski. 2005. Pex3p initiates the formation of a preperoxisomal compartment from a subdomain of the endoplasmic reticulum in *Saccharomyces cerevisiae. J. Biol. Chem.* 280:34933–34939. doi:10.1074/jbc.M506208200.

Titorenko, V.I., and R.A. Rachubinski. 1998. Mutants of the yeast *Yarrowia lipolytica* defective in protein exit from the endoplasmic reticulum are also defective in peroxisome biogenesis. *Mol. Cell. Biol.* 18:2789–2803.

Titorenko, V.I., G.A. Eitzen, and R.A. Rachubinski. 1996. Mutations in the *PAY5* gene of the yeast *Yarrowia lipolytica* cause the accumulation of multiple subpopulations of peroxisomes. *J. Biol. Chem.* 271:20307–20314. doi:10.1074/jbc.271.34.20300.

Titorenko, V.I., D.M. Ogrydziak, and R.A. Rachubinski. 1997. Four distinct secretory pathways serve protein secretion, cell surface growth, and peroxisome biogenesis in the yeast *Yarrowia lipolytica. Mol. Cell. Biol.* 17:5210–5226.

Titorenko, V.I., H. Chan, and R.A. Rachubinski. 2000. Fusion of small peroxisomal vesicles in vitro reconstructs an early step in the in vivo multistep peroxisome assembly pathway of *Yarrowia lipolytica. J. Cell Biol.* 148:29–44. doi:10.1083/jcb.148.1.29.

van den Bosch, H., R.B.H. Schutgens, R.J.A. Wanders, and J.M. Tager. 1992. Biochemistry of peroxisomes. *Annu. Rev. Biochem.* 61:157–197. doi:10.1146/annurev.bi.61.070192.001105.

Vizeacoumar, F.J., J.C. Torres-Guzman, Y.Y.C. Tam, J.D. Aitchison, and R.A. Rachubinski. 2003. *YHR150w* and *YDR479c* encode peroxisomal integral membrane proteins involved in the regulation of peroxisome number, size, and distribution in *Saccharomyces cerevisiae. J. Cell Biol.* 161:321–332. doi:10.1083/jcb.200210130.

Wanders, R.J.A., and H.R. Waterham. 2006. Biochemistry of mammalian peroxisomes revisited. *Annu. Rev. Biochem.* 75:295–332. doi:10.1146/annurev.biochem.74.082803.133329.

Weisman, L.S. 2006. Organelles on the move: insights from yeast vacuole inheritance. *Nat. Rev. Mol. Cell Biol.* 7:243–252. doi:10.1038/nrm1892.

Weisman, L.S., R. Bacallao, and W. Wickner. 1987. Multiple methods of visualizing the yeast vacuole permit evaluation of its morphology and inheritance during the cell cycle. *J. Cell Biol.* 105:1539–1547. doi:10.1083/jcb.105.4.1539.

Yan, M., D.A. Rachubinski, S. Joshi, R.A. Rachubinski, and S. Subramani. 2008. Dysferlin domain-containing proteins, Pex30p and Pex31p, localized to two compartments, control the number and size of oleate-induced peroxisomes in *Pichia pastoris. Mol. Biol. Cell.* 19:885–898. doi:10.1091/mbc.E07-10-1042.